Neuropathic and inflammatory pain are modulated by tuberoinfundibular peptide of 39 residues

Eugene L. Dimitrov[a], Jonathan Kuo[a], Kenji Kohno[b], and Ted B. Usdin[a,1]

[a]Section on Fundamental Neuroscience, National Institute of Mental Health, Bethesda, MD 20892; and [b]Laboratory of Molecular and Cell Genetics, Graduate School of Biological Sciences, Nara Institute of Science and Technology, Ikoma Nara 630-0192, Japan

Edited* by Tomas G. M. Hökfelt, Karolinska Institutet, Stockholm, Sweden, and approved June 28, 2013 (received for review April 4, 2013)

Nociceptive information is modulated by a large number of endogenous signaling agents that change over the course of recovery from injury. This plasticity makes understanding regulatory mechanisms involved in descending inhibition of pain scientifically and clinically important. Neurons that synthesize the neuropeptide TIP39 project to many areas that modulate nociceptive information. These areas are enriched in its receptor, the parathyroid hormone 2 receptor (PTH2R). We previously found that TIP39 affects several acute nociceptive responses, leading us to now investigate its potential role in chronic pain. Following nerve injury, both PTH2R and TIP39 knockout mice developed less tactile and thermal hypersensitivity than controls and returned to baseline sensory thresholds faster. Effects of hindpaw inflammatory injury were similarly decreased in knockout mice. Blockade of α-2 adrenergic receptors increased the tactile and thermal sensitivity of apparently recovered knockout mice, returning it to levels of neuropathic controls. Mice with locus coeruleus (LC) area injection of lentivirus encoding a secreted PTH2R antagonist had a rapid, α-2 reversible, apparent recovery from neuropathic injury similar to the knockout mice. Ablation of LC area glutamatergic neurons led to local PTH2R-ir loss, and barley lectin was transferred from local glutamatergic neurons to GABA interneurons that surround the LC. These results suggest that TIP39 signaling modulates sensory thresholds via effects on glutamatergic transmission to brainstem GABAergic interneurons that innervate noradrenergic neurons. TIP39's normal role may be to inhibit release of hypoalgesic amounts of norepinephrine during chronic pain. The neuropeptide may help maintain central sensitization, which could serve to enhance guarding behavior.

supraspinal pain | allodynia | partial sciatic nerve ligation | Freund's adjuvant

Nociceptive information entering the central nervous system (CNS) is modulated by projections from more rostral regions. Changes in this descending inhibition, or facilitation, are part of the normal homeostatic response to injury. CNS plasticity may also contribute to pain that sometimes persists after tissue damage is repaired. This type of chronic pain remains a significant clinical problem, motivating increased understanding of descending pain modulation.

Norepinephrine is one of several pain modulatory transmitters released in the spinal cord dorsal horn (1–3). It inhibits pain transmission through presynaptic α-2A adrenergic receptors on primary nociceptive afferents and postsynaptic α-2C receptors on GABA interneurons (4). Activation of these receptors may contribute to the efficacy of α-2 adrenergic receptor agonists and norepinephrine uptake inhibitors (e.g., tricyclic antidepressants) in some painful conditions (5–8). Endogenous norepinephrine transmission does not affect baseline sensory thresholds, but its increased release during sustained pain is antinociceptive (9). Noradrenergic fibers in the spinal cord originate mainly in the pontine locus coeruleus (LC; A6) with some contributions from the brainstem A5 and A7 cell groups (10). The control of LC activity and its contribution to antinociception are not well understood.

We recently found that the neuropeptide tuberoinfundibular peptide of 39 residues (TIP39) modulates acute nociception (11). TIP39 is synthesized in only a few anatomically circumscribed groups of neurons that project to widespread regions that contain its receptor, the parathyroid hormone 2 receptor (PTH2R) (12–14). Many of these regions process pain information. Central administration of TIP39 is pronociceptive (15), whereas the absence of TIP39 signaling, in TIP39 knockout (KO) mice, mice with null mutation of the PTH2R, or following acute PTH2R block, reduces nocifensive responses in animal models of acute thermal and inflammatory pain (11). In this study, we followed up on these observations by investigating the potential role of TIP39 signaling in chronic pain models. We used partial sciatic nerve ligation (PNL) as an animal model for neuropathic pain and hind paw injection of complete Freund's adjuvant (CFA) as a model of chronic inflammatory pain. Investigation of the substantially reduced thermal hypersensitivity and tactile allodynia observed in mice without TIP39 signaling led to evidence suggesting that endogenous TIP39 regulates descending inhibition of pain, likely through inhibition of LC neurons.

Results

We first examined the effect of a model neuropathic injury on mice without TIP39 signaling. As expected, WT mice developed pronounced thermal hyperesthesia and tactile allodynia by the fifth day following PNL. Thermal hyperesthesia persisted for approximately 40 d, whereas mechanical allodynia lasted at least 60 d after PNL, and often to the experimental endpoint at 80 d. The greatest thermal and tactile sensitivity was on the 10th postsurgical day (Fig. 1 *A*, *D*, *G*, and *J*). In striking contrast, PTH2R-KO mice did not develop thermal hypersensitivity following PNL (Fig. 1*B*). Their mechanical sensitivity followed the same pattern over time as WT but was somewhat less at all time points, including the 10th postsurgical day (Fig. 1*E*). The increased mechanical sensitivity of PTH2R-KO mice did not reach statistical significance at any time and returned to the level of uninjured mice at a time that WT still had significant allodynia (Fig. 1 *D* and *E*). The nociceptive phenotype of TIP39-KO mice was similar to the PTH2R-KO. TIP39-KO mice did not develop thermal hypersensitivity (Fig. 1*H*), and their increased mechanical sensitivity lasted for approximately 30 d (Fig. 1*K*), whereas the corresponding WT group still had significant tactile allodynia at the experiment's endpoint, 80 d (Fig. 1*J*). Area under the curve measurements indicate that PTH2R-KO and TIP39-KO mice differed significantly from WT in thermal and mechanical sensitivity following PNL (Fig. 1 *C*, *F*, *I*, and *L*).

Next, we examined the effect of TIP39 signaling loss using the CFA model of chronic inflammatory pain. As expected, hindpaw CFA injection increased both thermal and tactile sensitivity of WT

Author contributions: E.L.D. and T.B.U. designed research; E.L.D. and J.K. performed research; K.K. and T.B.U. contributed new reagents/analytic tools; E.L.D. and T.B.U. analyzed data; and E.L.D. and T.B.U. wrote the paper.

The authors declare no conflict of interest.

*This Direct Submission article had a prearranged editor.

[1]To whom correspondence should be addressed. E-mail: usdint@mail.nih.gov.

This article contains supporting information online at www.pnas.org/lookup/suppl/doi:10.1073/pnas.1306342110/-/DCSupplemental.

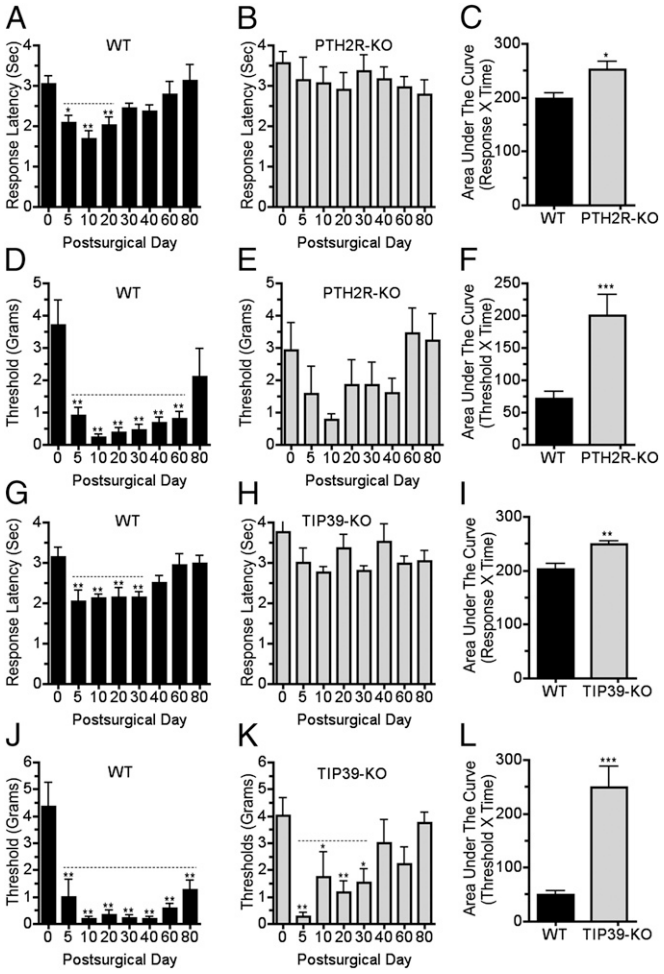

Fig. 1. Mice without TIP39 signaling develop less thermal hypersensitivity and tactile allodynia following nerve injury than WT. Thermal and mechanical hindpaw withdrawal thresholds were measured over time following PNL of PTH2R-KO (*A–F*) and TIP39-KO (*G–L*) mice and WT littermates. WT developed thermal hypersensitivity that lasted for 20 (*A*; $F_{7, 56} = 5.8$; $P < 0.001$) to 30 d (*G*; $F_{7, 49} = 5.4$; $P < 0.01$). PTH2R-KO (*B*) and TIP39-KO (*H*) did not develop significant thermal hypersensitivity. Area under the curve measurements for the total experiment duration showed significant differences between thermal sensitivity of WT and both PTH2R-KO (*C*; $P < 0.05$, $n = 7–9$ per group) and TIP39-KO (*I*; $P < 0.01$, $n = 7–8$ per group). PNL caused mechanical hypersensitivity (allodynia) in WT that lasted from 60 (*D*; $F_{7, 56} = 7.8$; $P < 0.001$) to at least 80 (*J*; $F_{7, 49} = 11.5$; $P < 0.001$) days, the experiment's endpoint. Mechanical withdrawal thresholds of PTH2R-KO mice did not significantly differ from baseline at any time (*E*). TIP39-KO mice developed allodynia lasting 30 d (*K*; $F_{7, 49} = 3.1$; $P < 0.001$). Area under the curve measurements showed that PTH2R-KO (*F*; $P < 0.001$, $n = 7–9$ per group) and TIP39-KO (*L*; $P < 0.001$, $n = 7–8$ per group) developed significantly less mechanical sensitivity than WT. Dotted lines indicate time over which withdrawal thresholds differed significantly from the presurgical value. *P* values in the legend correspond to the effect of time in the ANOVA. Symbols above the columns are from the post hoc test. $*P < 0.05$, $**P < 0.01$, $***P < 0.001$.

mice. Thermal hyperesthesia lasted for approximately 4 d and mechanical allodynia for more than 20 d (Fig. 2 *A* and *D*). PTH2R-KO mice developed less hyperesthesia and allodynia, and their increased tactile sensitivity lasted for only about half as long as that of WT (Fig. 2 *B* and *E*). There were significant genotype differences in both mechanical and thermal sensitivity following CFA (Fig. 2 *C* and *F*).

Paw withdrawal from thermal or tactile stimuli is primarily a spinal reflex. It is modulated by brain activity, but does not necessarily reflect conscious aspects of pain and may not be optimal for assessing the types of pain that are most disturbing to humans. Tests that use observation of spontaneous or motivated behavior may be better suited for assessment of emotional-affective components of pain. However, it has been difficult to identify changes in behavior of mice that are expected to be experiencing pain. Recently, Clifford Woolf and coworkers developed a paradigm in which they observed decreased voluntary wheel running in mice following hindpaw CFA injection (16). We adapted this procedure to compare wheel-running activity of WT and PTH2R-KO mice. Following 3 d of 24-h-per-day access, running wheels were placed in the home cages for 1 h per day for the duration of the experiment. (Baseline running did not differ between the genotypes in this experiment or in ones in which mice were given unlimited running wheel access for several weeks.) After the third day of 1-h access, both hind paws were injected with 20 μL of CFA. CFA injection decreased the running behavior of WT for 2 d but did not have a significant effect on behavior of the PTH2R-KO mice (Fig. 3 *A* and *B*).

We also compared guarding behavior between WT and PTH2R-KO mice following PNL, using a static weight bearing test. The test compared weight distribution between the left (injured) and right (uninjured) hind leg of animals in the upright position. Animals with increased nociception in one leg tend to favor the opposite side and shift their body weight to the uninjured limb. This guarding behavior lasted for approximately 20 d following PNL surgery in WT mice (Fig. 3*C*). PTH2R-KO did not exhibit any significant weight shift away from the injured leg (Fig. 3*D*).

To address the mechanism underlying the decreased pain-like behavior of the KO mice, we examined the effects of drugs that block endogenous pain modulatory systems. Previously, we observed that CB-1 cannabinoid receptor block eliminates differences between mice with and without TIP39 signaling in acute nociceptive tests (11). We initially examined the effect of antagonist drugs on mechanical sensitivity of TIP39-KO mice 60 d following PNL. Contrary to expectation, neither cannabinoid CB1 receptor

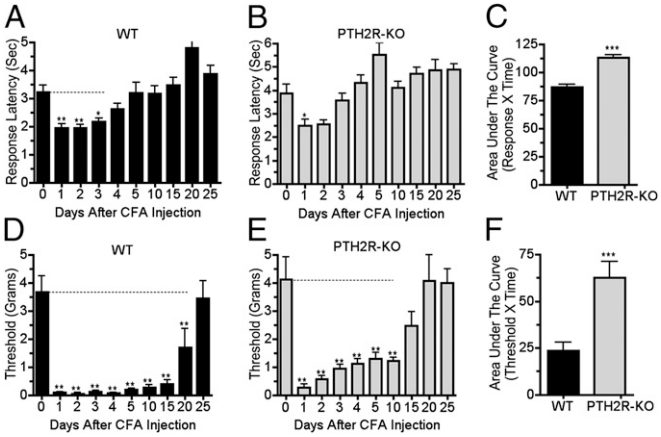

Fig. 2. PTH2R KO mice develop less thermal hypersensitivity and less tactile allodynia than WT in a chronic inflammatory injury model. Thermal and mechanical hindpaw withdrawal thresholds of PTH2R-KO and WT mice were evaluated over time following unilateral hindpaw injection of 20 μL of CFA. WT had thermal hypersensitivity on days 1–3 following injection (*A*; $F_{9, 81} = 11.8$; $P < 0.001$) but thermal sensitivity of PTH2R-KO mice was only significantly increased on day 1 (*B*; $F_{9, 63} = 8.1$; $P < 0.001$). Mechanical allodynia lasted for 20 d after CFA injection in WT (*D*; $F_{9, 81} = 17.8$; $P < 0.001$) but only for 10 d in PTH2R-KO (*E*; $F_{9, 63} = 12.4$; $P < 0.001$). Area under the curve measurements over the total experiment duration indicated significant differences between the thermal (*C*; $P < 0.001$, $n = 8–10$ per group) and mechanical (*F*; $P < 0.001$, $n = 8–10$ per group) sensitivities of WT and PTH2R-KO. Dotted lines indicate times over which withdrawal thresholds differed significantly from the presurgical value. *P* values in the legend refer to the effect of time. Symbols above the columns refer to the post hoc test. $*P < 0.05$, $***P < 0.001$.

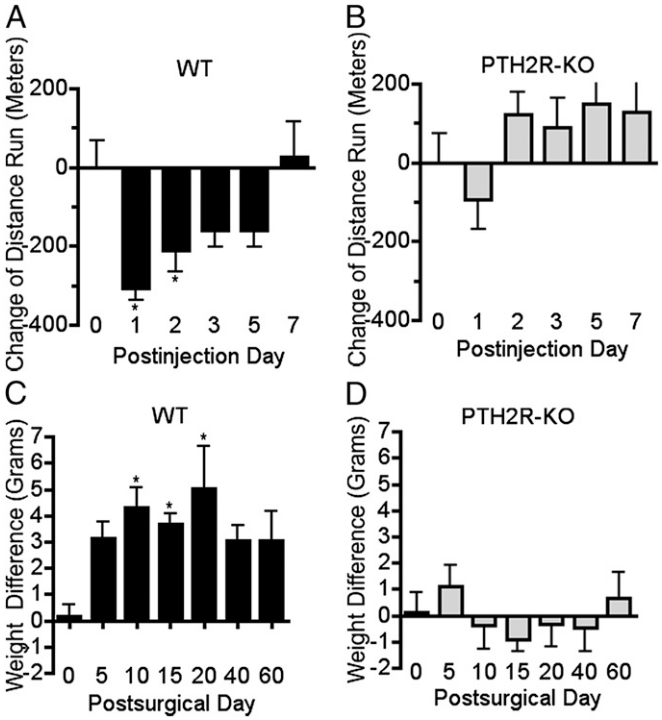

Fig. 3. PTH2R-KO mice display less spontaneous nocifensive behavior in chronic inflammatory and nerve injury models. Wheel running following hindpaw CFA injection and static hindpaw weight bearing after PNL were compared between WT and PTH2R-KO mice. (*A* and *B*) Change in running wheel activity with 1-h daily access following bilateral hindpaw injection of 20 μL of CFA. The distance run by WT decreased significantly for 2 d (*A*; $F_{5, 25} = 7.5$; $P < 0.001$), whereas the effect of CFA on PTH2R-KO running was not significant (*B*; $F_{5, 25} = 1.9$; $P > 0.05$). (*C* and *D*) Hindpaw static weight bearing following unilateral PNL. Guarding behavior, demonstrated by reduced injured side weight bearing, lasted for 20 d following PNL in WT mice (*C*; $F_{6, 60} = 2.4$; $P < 0.05$), whereas the PTH2R-KO mice had no weight bearing shift (*D*). *P* values in the legend refer to the effect of time in the ANOVA. Symbols above the columns refer to the post hoc test. $^{*}P < 0.05$, $^{**}P < 0.01$.

block with rimonabant nor opioid receptor block with naloxone affected the difference in mechanical sensitivity between WT and TIP39-KO mice (Fig. 4*A*). However, the α-2 adrenergic receptor blocker yohimbine dramatically increased the sensitivity of TIP39-KO mice (Fig. 4*A*). The thermal hypersensitivity of the WT mice had diminished at the time of this experiment. We next performed a similar experiment in PTH2R-KO mice 40 d following PNL, when there was a significant difference in both thermal and mechanical sensitivity between WT and KO mice. i.p. yohimbine and intrathecal atipamezole decreased both the thermal and mechanical thresholds in PTH2R-KO animals (indicating return of hypersensitivity caused by the nerve injury) (Fig. 4 *B*–*E*).

Based on our understanding of the literature (e.g., refs. 17 and 18), the most likely site and source of α-2 adrenergic–mediated antinociception is norepinephrine released in the spinal cord dorsal horn from projections of LC or other brainstem noradrenergic neurons. Fibers containing TIP39 and PTH2R immunoreactivity are present in many pain regulatory regions, including the LC and more rostral regions that influence the LC, such as the central amygdala (CAmy). We targeted stereotaxic injections of a lentivirus encoding a secreted PTH2R antagonist (HYWH-lenti) to the CAmy and LC of WT mice. CAmy infection by HYWH-lenti did not affect development of thermal and tactile hypersensitivity in mice with PNL (Fig. S1). Like the KOs, mice with PNL and LC area HYWH-lenti injection developed less thermal hypersensitivity than control animals, and their hypersensitivity lasted for a shorter time (Fig. 5 *A* and *B*). Mice injected with the control (GFP only) virus developed allodynia, as expected (Fig. 5*D*). Mechanical sensitivity of mice with LC-targeted HYWH-lenti varied widely, but changes did not reach statistical significance at any time during the first 40 d after PNL (Fig. 5*E*). As observed in KO mice, yohimbine significantly increased the thermal and mechanical sensitivity of mice with LC-directed HYWH-lenti and PNL, when administered at a time that they significantly differed from lesioned controls (Fig. 5 *G* and *H*). The time course of thermal and mechanical sensitivity of HYWH-lenti–injected mice differed somewhat from other experimental groups. Surprisingly, HYWH-lenti mice developed significant thermal hypersensitivity and mechanical allodynia between the 40th and 60th postsurgical days, which increased at 80 d, the last time point examined (Fig. S2 *A* and *B*). HYWH-lenti also encodes GFP. Mice euthanized 80 d after

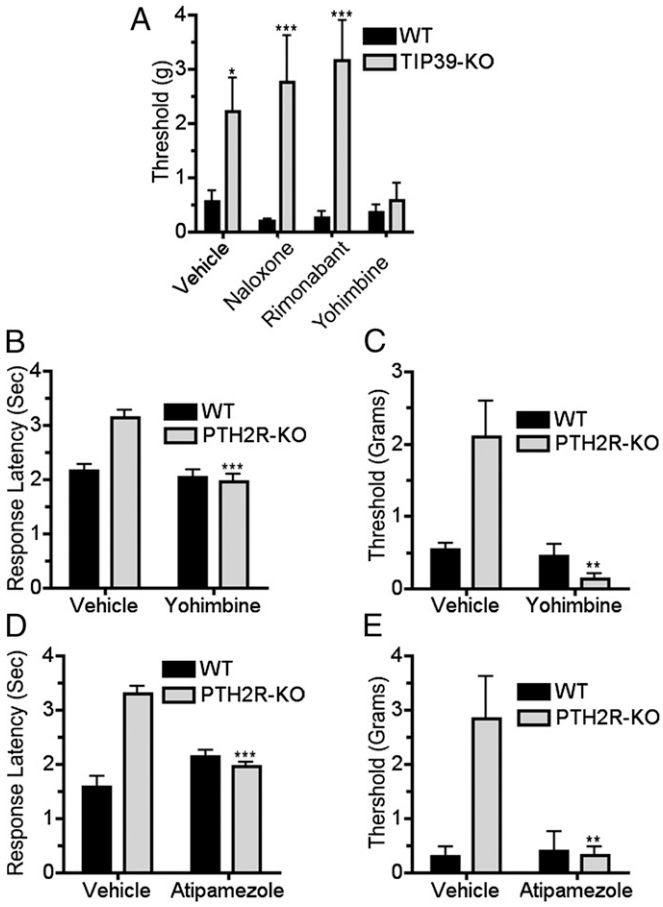

Fig. 4. α-2 adrenergic block reverses the apparent recovery of nerve-injured TIP39-KO and PTH2R-KO mice. The opioid antagonist naloxone (5 mg/kg i.p.) and the cannabinoid antagonist rimonabant (5 mg/kg i.p.) did not change the mechanical sensitivity of TIP39-KO mice 60 d after nerve injury, but the adrenergic blocker yohimbine (2.5 mg/kg i.p.) decreased the mechanical threshold to the WT level (*A*; $F_{3, 49} = 15.4$, $P < 0.05$ for interaction, $F_{1, 49} = 47.2$, $P < 0.001$ for genotype and $F_{3, 49} = 12.9$, $P < 0.05$ for treatment as measured by two-way ANOVA. Bonferroni post hoc test showed significant differences between "no treatment" groups, $P < 0.05$, "naloxone" $P < 0.001$, and "rimonabant" groups $P < 0.001$ but not between "yohimbine" treated groups, $P > 0.05$). Thermal and mechanical withdrawal thresholds of WT and PTH2R-KO mice were also evaluated 40 d following PNL with, or without, α-2 adrenergic antagonist administration. Yohimbine (2.5 mg/kg i.p.) increased the thermal (*B*; $F_{1, 44} = 14.5$, $P < 0.001$) and mechanical (*C*; $F_{1, 44} = 10.4$, $P < 0.01$) sensitivity of injured PTH2R-KO mice, bringing it to the level of neuropathic WT. Intrathecal α-2 adrenergic receptor blocker (atipamezole, 0.3 mg/kg) produced a similar reversal of the apparent recovery of PTH2R-KO mice from thermal (*D*; $F_{1, 18} = 43.7$, $P < 0.001$) and mechanical hypersensitivity (*E*; $F_{1, 18} = 9.4$, $P < 0.01$).

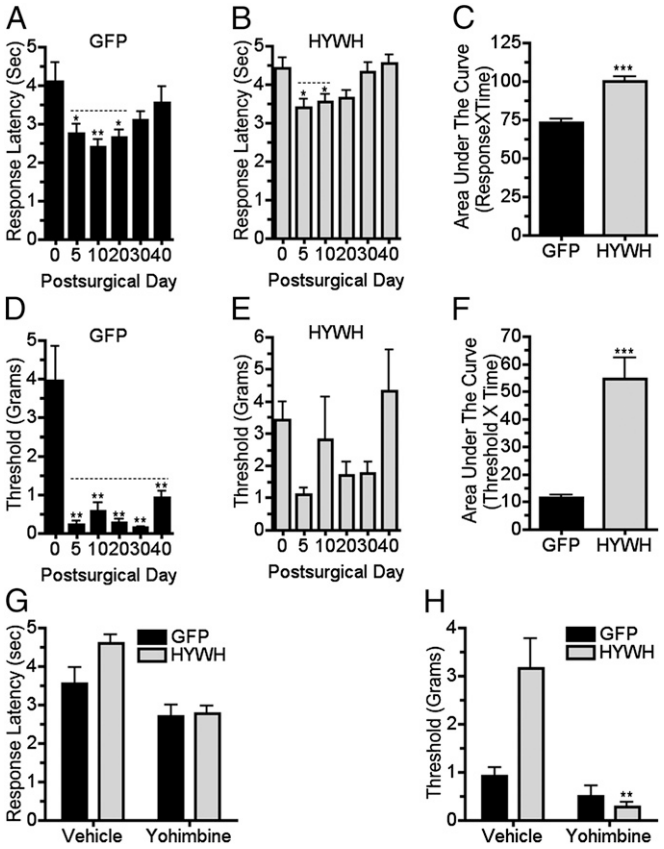

Fig. 5. Brainstem delivery of a PTH2R antagonist reduces development of mechanical hypersensitivity following nerve injury. Thermal and mechanical withdrawal thresholds were measured following PNL in mice with LC-targeted injection of a PTH2R antagonist-coding virus. Control virus (GFP) injected mice had increased thermal sensitivity (*A*; $F_{5, 41} = 3.9$; $P < 0.01$) that was significantly different from their presurgical sensitivity for 30 d following surgery. Mice injected with antagonist encoding virus (HYWH) had increased thermal sensitivity (*B*; $F_{5, 83} = 4.9$; $P < 0.001$) for only 20 d. Increased mechanical sensitivity after PNL in control virus-injected mice (*D*; $F_{5, 41} = 14.4$; $P < 0.001$) lasted for 40 d but was not significant in HYWH-injected mice (*E*; $F_{5, 83} = 2.2$; $P > 0.05$). Area under the curve measurements over the 40-d experimental period indicated significant differences between thermal (*C*; $P < 0.001$, $n = 7$–14 per group) and mechanical (*F*; $P < 0.001$, $n = 7$–14 per group) sensitivities of mice injected with the control and antagonist viruses. Yohimbine administration (2.5 mg/kg i.p.), 40 d following PNL, significantly increased the thermal (*G*; $F_{1, 38} = 21.7$, $P < 0.001$) and mechanical (*H*; $F_{1, 38} = 14.1$, $P < 0.001$) sensitivity of mice injected with antagonist virus before surgery, bringing their sensitivity to the level of control virus-injected neuropathic mice. Statistical comparison showed significant interaction between virus and drug administration only for the mechanical thresholds (*H*; $F_{1, 38} = 7.8$, $P < 0.01$). *P* values in legend refer to effect of time and symbols above the columns refer to post hoc tests. For drug treatments, *P* values in the legend refer to virus × drug interaction. $*P < 0.05$, $**P < 0.01$, $***P < 0.001$.

PNL, which was more than 100 d after virus injection, had only traces of GFP labeling in the LC area (Fig. S2 *D* and *F*). Mice euthanized 3 wk after LC-targeted HYWH-lenti injection had strong GFP expression, suggesting that virus expression or virus expressing cells were lost at a later time (Fig. S2 *C* and *E*).

In several brain regions, PTH2Rs have been shown to be located on glutamatergic nerve terminals (11, 19). We found that this colocalization is also the case in the LC area. To better understand the distribution of VGlut2- and PTH2R-expressing cells in the LC area, we immunolabeled TH in sections from mice in which a population of glutamatergic neurons contained red fluorescent protein (VGlut2cre-tdTomato) or PTH2R expressing neurons contained GFP (PTH2R-cre-GFP). Both VGlut2cre-tdTomato and PTH2R-cre-GFP containing cells were abundant near TH-ir neurons and dispersed within pericoerulear areas, as demarcated by a network of TH-ir processes (Fig. S3). Because the PTH2R antibody labels fibers and terminals but not cell bodies, we evaluated PTH2R immunolabeling in brain sections from VGlut2cre-tdTomato mice. There was a high level of colocalization between PTH2R-ir and VGlut2cre-tdTomato terminals in the LC area (Figs. S3 and S4). There was also a substantial decrease of PTH2R-ir fibers in the LC area following diphtheria toxin-mediated local ablation of VGlut2 expressing neurons, confirming that fibers with PTH2R and glutamatergic markers belong to the same local neuronal population and are not terminals of projection neurons from another brain region (Fig. S5).

To evaluate the connectivity of LC area glutamatergic neurons, we injected AAV that encoded Cre-dependent expression of barley lectin (a protein similar to, and immuno-cross-reactive with, wheat germ agglutinin, which is also anterogradely transported between neurons; ref. 20) into the LC area of VGlut2-Cre mice. Many LC area neurons, including some within the pericoerulear area, contained barley lectin immunoreactivity (BL-ir). The population of labeled neurons extended ventrally to the seventh cranial nerve, to the medial parabrachial nucleus laterally, and Barrington nucleus medially. BL-ir was completely restricted to the injection side (Fig. 6*A*). The dorsomedial hypothalamic nucleus and medial tuberal nucleus were the only structures outside the LC area that contained BL-ir (Fig. S6). Almost none of the LC noradrenergic neurons contained BL-ir, but numerous GABA-ir neurons surrounding the nucleus contained strong BL-ir (Fig. 6 *B*–*E*). This labeling strongly argues that local glutamatergic neurons innervate LC area GABAergic neurons.

Discussion

The major finding of this study is that mice without TIP39 signaling develop significantly less nociceptive sensitivity than control animals following nerve or chronic inflammatory injury. This hyposensitivity appears to result from development of greater noradrenergic signaling in the spinal cord following injury. The data are consistent with the suggestion that TIP39 acts via glutamatergic neurons near the LC to modulate the function of spinal cord projecting noradrenergic neurons. The difference in nociception between WT and KO mice was reflected in wheel

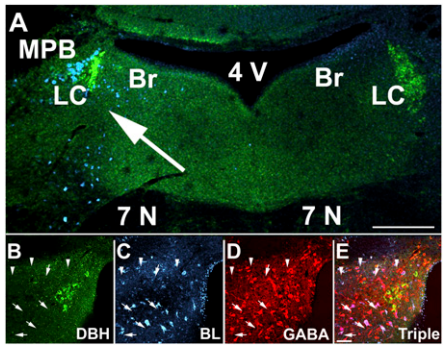

Fig. 6. Evidence for local glutamatergic innervation of LC area GABAergic neurons. VGlut2-ires-Cre mice were unilaterally injected near the LC with AAV encoding Cre-dependent barley lectin 3 wk before they were euthanized, and sections through the LC area were labeled with antibodies to dopamine beta hydroxylase (DBH, green), BL (cyan), and GABA (red). Note the distribution of BL-ir on the virus-injected side (*A*, arrow). *B*–*E* show high magnification images of DBH-ir (*B*), BL-ir (*C*), GABA-ir (*D*), and a merged image (*E*). Arrows point to multiple GABA neurons surrounding the LC and colocalized BL-ir. Arrowheads point to non-GABAergic neurons colocalized with BL-ir. None of the DBH-ir neurons shown on this section contain BL-ir. 4V, fourth ventricle; 7N, seventh cranial nerve; BR, Barrington nucleus; LC, locus ceruleus; MPB, medial parabrachial nucleus. (Scale bars: *A*, 200 μm; *B*–*E*, 20 μm.)

running behavior and weight bearing, which may be more analogous to pain than measures based on spinal reflexes.

Localization of TIP39 modulation of nociception to the LC in the neuropathic and chronic inflammatory pain models is based on: (*i*) α-2-adrenergic dependency of the relative hypoalgesia of mice without TIP39 signaling, (*ii*) replication of this phenotype of TIP39- and PTH2R-KO mice by LC-directed injection of a PTH2R antagonist encoding virus, and (*iii*) the presence of PTH2Rs and TIP39 containing fibers near the LC. Although noradrenergic signaling is widespread, the spinal cord dorsal horn is the only site where we are aware that α-2-adrenergic signaling has an antinociceptive action, and spinal cord norepinephrine is released from terminals of brainstem noradrenergic neurons (3). Spinal cord location of the noradrenergic signaling is supported by efficacy of an intrathecally delivered α-2 antagonist. We assign the TIP39 signaling to the LC instead of other pontine noradrenergic nuclei because, in most reports, the LC is the major source of spinal cord dorsal horn noradrenergic fibers that influence nociception (10), the LC is enriched in PTH2Rs, and LC-directed injection of an antagonist-encoding virus mimics the phenotype of KO mice. None of these criteria are definitive. We do not know the effective diffusion distance of the secreted PTH2R antagonist, and the relative contribution of brainstem noradrenergic nuclei to spinal antinociception varies between reports, likely due to species or strain differences (21, 22). However, the A7 group is unlikely to mediate TIP39 effects because there are very few PTH2Rs in its vicinity. The A5 group contains PTH2Rs and TIP39 fibers, but its major projection is to the intermediolateral cell column and its fibers do not reach the lumbar spinal cord where sciatic nerve afferents synapse (22). The LC is influenced by projections from more rostral areas that affect nociception including the periaqueductal gray (23) and amygdala (24–26). TIP39 signaling in the amygdala seems unlikely to be relevant because CAmy-directed injection of HYWH-lenti was not effective, but other brain regions cannot be completely excluded.

PTH2Rs are enriched in the spinal cord dorsal horn. TIP39 action there is not completely excluded, but there are strong arguments against it. Very little TIP39 can be detected in the area and, to explain the results, the antagonist would need to reach the lumbar dorsal horn from pontine cells that secrete it. Although the antagonist's effective diffusion distance is unknown, this distance seems unlikely. The antagonist does not reach an effective site following amygdala infection.

The pontine PTH2Rs are expressed by local glutamatergic neurons and terminals, and we speculate that their activation by TIP39 results in augmented glutamate release from presynaptic terminals. Transfer of barley lectin from LC area glutamatergic neurons to nearby GABAergic neurons suggests a potential mechanism for TIP39 modulation of LC activity and descending pain inhibition. Glutamate release potentiated by TIP39 may increase activation of GABA interneurons with subsequent inhibition of LC noradrenergic neurons and suppression of spinal norepinephrine release. This particular pool of GABA neurons and their innervation of LC neurons has been demonstrated by retrograde viral labeling (27). Communication of TIP39 signaling through GABA interneurons is consistent with the observed effects on pain behavior and barley lectin transfer. It is somewhat surprising because of PTH2R/VGlut2 colocalization within the LC nuclear zone. Barley lectin may not transfer between all connected neurons with equal efficiency, and other mechanisms to consider for TIP39 modulation of nociception include ones related to postactivation inhibition (28) or increased release of norepinephrine that acts via presynaptic autoreceptors or somatodendritic α-2 receptors on neighboring noradrenergic neurons to inhibit their activity (29). A testable hypothesis that is common to these hypothetical mechanisms is that global or local loss of TIP39 signaling has a disinhibitory effect on LC electrical activity. The precise mechanisms underlying the hypothesized sustained activation of local glutamatergic neurons during chronic pain are not known, and entirely different mechanisms for TIP39's action are plausible.

These results suggest that endogenous TIP39 signaling inhibits LC-derived antinociception during periods of prolonged pain. TIP39 is likely to be one of many LC modulators, and norepinephrine is one of several transmitters that contribute to descending pain modulation, so elucidation of the physiological role and significance of this pathway will require significantly more investigation. We speculate that the biological advantage of increased pain perception caused by a neuropeptide projecting to the LC is that it fosters guarding behavior and, in this way, promotes healing. This work raises the question of whether a PTH2R antagonist may be useful in treating pain.

Materials and Methods

Animals. Procedures were approved by the National Institute of Mental Health (NIMH) Animal Care and Use Committee and in accordance with the Institute for Laboratory Animal Research Guide for the Care and Use of Laboratory Animals. Male WT and KO mice from the same Het × Het breedings, initially 80–120 d old, 28–32 g, were singly housed following surgery and for experiments. Testing in the morning followed at least 1 h of acclimatization to the testing room. TIP39 (30) and PTH2R-KO (11) mice have been described. VGlut2-ires-Cre mice (31), from Bradford Lowell (Center for Life Sciences, Beth Israel Deaconess Medical Center, Boston, MA) were bred with reporter mice (B6.Cg-*Gt(ROSA)26Sor*$^{tm9(CAG\text{-}tdTomato)Hze}$/J; ref. 32) to express red fluorescent protein in VGlut2-expressing glutamatergic neurons (VGlut2cre-tdTomato). PTH2R-Cre mice were produced in the NIMH transgenic core by embryo injection of a bacterial artificial chromosome with the first PTH2R coding exon replaced by Cre recombinase and bred with reporter mice (Gt(ROSA)26Sor$^{tm1.1(CAG\text{-}EGFP)Fsh}$; ref. 33) to express GFP in neurons that normally express PTH2Rs (PTH2Rcre-GFP).

Virus Preparation. HYWH-GFP lentivirus was designed to express a secreted form of histidine[4], tyrosine[5], tryptophan[6], histidine[7]-TIP39 (HYWH-TIP39), a PTH2R antagonist (34), plus cytoplasmic GFP. A control virus expressed GFP only. HYWH-GFP lentivirus was produced by combined oligonucleotide synthesis, PCR, and conventional subcloning. The resulting construct encoded the fibronectin signal sequence followed by HYWH-TIP39 sequence, then an IRES sequence, and finally GFP sequence. Following transfer to pWPI (Addgene 12254; D. Trono, École Polytechnique Fédérale de Lausanne, Lausanne, Switzerland), viral particles were produced in HEK293T cells by using psPAX2 (Addgene 12260; D. Trono), and pMD2.G (Addgene 12259; D. Trono), and concentrated by polyethylene glycol precipitation and ultracentrifugation (35). Virus encoding only GFP was produced from pFUGW-GFP (Addgene 14883; ref. 36; D. Baltimore, California Institute of Technology, Pasadena, CA). AAV encoding a Cre recombinase dependent human diphtheria toxin receptor was produced by subcloning from pTRECK6 (37) into pj241 Flex (Addgene 18925; ref. 38), and then into pFBGR (gift of Robert Kotin, National Heart, Lung, and Blood Institute, Bethesda, MD). AAV particles (serotype 8; AAV-FLEX-DTR) were produced as described by Cecchini et al. (39). AAV encoding Cre-dependent barley lectin (20) expression was produced similarly. Construct sequences were confirmed by using the National Institute of Neurological Disorders and Stroke intramural sequencing facility.

Nociceptive Tests. Hindpaw thermal sensitivity ("Hargreaves" test) was measured after mice were left undisturbed in individual compartments on a glass platform for 15–20 min. A light beam with preset intensity of 80% (Analgesia Meter Model 390; IITC Life Science) was directed to the injured paw at a moment the animal was calm and nonmoving. A manual timer was stopped at the moment of vigorous lift, shake, or biting of the heat-exposed paw. Tactile sensitivity was measured by using von Frey filaments (North Coast Medical), and the 50% threshold was calculated by Dixon's up and down method (40) as described by Chaplan et al. (41).

Spontaneous Activity After CFA injection. Wheel-running and weight-bearing tests were adapted from Cobos et al. (16). Mice were singly housed in standard rat cages for 1 wk, then telemetric running wheels (ENV-044; Med Associates) were placed in the cages continuously for 3 d followed by 1 h at the same time every day for the remainder of the experiment. Running activity on the third day of 1-h-per-day access was used as baseline activity. Both hindpaws then received 20 μL of CFA injections, and running activity was recorded on the next 7 d.

Mice were familiarized with the weight-bearing scale (Incapacitance Meter; Harvard Apparatus) in two 5-min sessions. Measurements were

obtained when animals were calm, the body elevated in prancing position, front paws touching the frontal surface of the box, and with both hindpaws on the scale surface at even distance from the edges of the scale. The average of three measurements was used as the measure of weight distribution.

Surgery. Intrathecal injections were performed under light isoflurane injection as described (42). Thermal and mechanical sensitivity were tested 30 min after injections. PNL surgery was performed under isoflurane anesthesia as described by Malmberg and Basbaum (43) by using 7-0 nonabsorbable monofilament polypropylene suture (Surgipro). Nociceptive tests were conducted on the fifth and 10th postsurgical day and at 10-d intervals after that for 80 d after the surgery. For LC area stereotaxic injection viruses (0.5 μL) were pressure injected by using a 30-gauge needle at anteroposterior −5.5 mm, lateral +1.0 mm relative to bregma, and 4.0 mm below the skull surface.

Immunohistochemistry. Immunohistochemistry was performed as described (44) on 40-μm vibratome sections. For the glutamatergic neuron ablation experiment, diphtheria toxin (500 ng i.p.; Sigma) was administered for 5 consecutive days starting 3 wk after AAV-FLEX-DTR injection, and mice were euthanized 12 d after the first injection. Labeling used rabbit anti-PTH2R (1:10,000; 0.1 μg/mL) detected with tyramide-mediated amplification (DyLight 488; Pierce) and sheep anti-TH (1:10,000; Neuromics) detected with an Alexa647 labeled secondary antibody (Jackson ImmunoResearch). Barley lectin was detected with goat anti-WGA (Vector Laboratories; 1:2,000) and amplification with AMCA-tyramide substrate, followed by labeling with mouse monoclonal anti-GABA antibody (1:1 000; SWANT) detected with Alexa564 anti-mouse (Jackson ImmunoResearch), and rabbit anti-dopamine beta hydroxylase (DBH) (1:1,000, Neuromics) detected with Alexa647 anti-rabbit antibody (Jackson ImmunoResearch). Sections were visualized by using a Zeiss LSM510 confocal microscope in the National Institute of Neurological Disorders and Stroke light microscope imaging facility.

Statistical Analysis. Data are presented as mean ± SEM. Student's *t* test was used for two group comparisons. Area under the curve was calculated from time course measurements for each animal individually by using the trapezoidal approximation method in Prism (GraphPad Software), and data were then grouped for statistical analysis. Time course data were evaluated by using one-way ANOVA with repeated measures followed by Dunnet's test comparing each time point with the presurgical response. Drug and genotype interaction were evaluated by using two-way ANOVA followed by Bonferroni post hoc test. The accepted level of significance was $P < 0.05$ in all tests.

ACKNOWLEDGMENTS. Technical support was provided by Milan Rusnak. Support was provided by the National Institute of Meantal Health Intramural Research Program.

1. Yaksh TL, Pogrel JW, Lee YW, Chaplan SR (1995) Reversal of nerve ligation-induced allodynia by spinal alpha-2 adrenoceptor agonists. *J Pharmacol Exp Ther* 272(1): 207–214.
2. Yaksh TL (1985) Pharmacology of spinal adrenergic systems which modulate spinal nociceptive processing. *Pharmacol Biochem Behav* 22(5):845–858.
3. Wei H, Pertovaara A (2006) Spinal and pontine alpha2-adrenoceptors have opposite effects on pain-related behavior in the neuropathic rat. *Eur J Pharmacol* 551(1-3): 41–49.
4. Stone LS, et al. (1998) Differential distribution of alpha2A and alpha2C adrenergic receptor immunoreactivity in the rat spinal cord. *J Neurosci* 18(15):5928–5937.
5. Eisenach JC, Gebhart GF (1995) Intrathecal amitriptyline. Antinociceptive interactions with intravenous morphine and intrathecal clonidine, neostigmine, and carbamylcholine in rats. *Anesthesiology* 83(5):1036–1045.
6. Esser MJ, Sawynok J (1999) Acute amitriptyline in a rat model of neuropathic pain: Differential symptom and route effects. *Pain* 80(3):643–653.
7. Hall FS, et al. (2011) A greater role for the norepinephrine transporter than the serotonin transporter in murine nociception. *Neuroscience* 175:315–327.
8. Bomholt SF, Mikkelsen JD, Blackburn-Munro G (2005) Antinociceptive effects of the antidepressants amitriptyline, duloxetine, mirtazapine and citalopram in animal models of acute, persistent and neuropathic pain. *Neuropharmacology* 48(2):252–263.
9. Rahman W, D'Mello R, Dickenson AH (2008) Peripheral nerve injury-induced changes in spinal alpha(2)-adrenoceptor-mediated modulation of mechanically evoked dorsal horn neuronal responses. *J Pain* 9(4):350–359.
10. Howorth PW, Teschemacher AG, Pickering AE (2009) Retrograde adenoviral vector targeting of nociresponsive pontospinal noradrenergic neurons in the rat in vivo. *J Comp Neurol* 512(2):141–157.
11. Dimitrov EL, Petrus E, Usdin TB (2010) Tuberoinfundibular peptide of 39 residues (TIP39) signaling modulates acute and tonic nociception. *Exp Neurol* 226(1):68–83.
12. Wang J, Palkovits M, Usdin TB, Dobolyi A (2006) Forebrain projections of tuberoinfundibular peptide of 39 residues (TIP39)-containing subparafascicular neurons. *Neuroscience* 138(4):1245–1263.
13. Wang J, Palkovits M, Usdin TB, Dobolyi A (2006) Afferent connections of the subparafascicular area in rat. *Neuroscience* 138(1):197–220.
14. Faber CA, Dobolyi A, Sleeman M, Usdin TB (2007) Distribution of tuberoinfundibular peptide of 39 residues and its receptor, parathyroid hormone 2 receptor, in the mouse brain. *J Comp Neurol* 502(4):563–583.
15. Dobolyi A, Ueda H, Uchida H, Palkovits M, Usdin TB (2002) Anatomical and physiological evidence for involvement of tuberoinfundibular peptide of 39 residues in nociception. *Proc Natl Acad Sci USA* 99(3):1651–1656.
16. Cobos EJ, et al. (2012) Inflammation-induced decrease in voluntary wheel running in mice: A nonreflexive test for evaluating inflammatory pain and analgesia. *Pain* 153(4):876–884.
17. Ossipov MH, Dussor GO, Porreca F (2010) Central modulation of pain. *J Clin Invest* 120(11):3779–3787.
18. Pertovaara A (2006) Noradrenergic pain modulation. *Prog Neurobiol* 80(2):53–83.
19. Dobolyi A, Irwin S, Wang J, Usdin TB (2006) The distribution and neurochemistry of the parathyroid hormone 2 receptor in the rat hypothalamus. *Neurochem Res* 31(2): 227–236.
20. Horowitz LF, Montmayeur JP, Echelard Y, Buck LB (1999) A genetic approach to trace neural circuits. *Proc Natl Acad Sci USA* 96(6):3194–3199.
21. Clark FM, Proudfit HK (1992) Anatomical evidence for genetic differences in the innervation of the rat spinal cord by noradrenergic locus coeruleus neurons. *Brain Res* 591(1):44–53.
22. Bruinstroop E, et al. (2012) Spinal projections of the A5, A6 (locus coeruleus), and A7 noradrenergic cell groups in rats. *J Comp Neurol* 520(9):1985–2001.
23. Bajic D, Proudfit HK (1999) Projections of neurons in the periaqueductal gray to pontine and medullary catecholamine cell groups involved in the modulation of nociception. *J Comp Neurol* 405(3):359–379.
24. Bernard JF, Bester H, Besson JM (1996) Involvement of the spino-parabrachio -amygdaloid and -hypothalamic pathways in the autonomic and affective emotional aspects of pain. *Prog Brain Res* 107:243–255.
25. Reyes BA, Carvalho AF, Vakharia K, Van Bockstaele EJ (2011) Amygdalar peptidergic circuits regulating noradrenergic locus coeruleus neurons: Linking limbic and arousal centers. *Exp Neurol* 230(1):96–105.
26. Viisanen H, Pertovaara A (2007) Influence of peripheral nerve injury on response properties of locus coeruleus neurons and coeruleospinal antinociception in the rat. *Neuroscience* 146(4):1785–1794.
27. Aston-Jones G, Zhu Y, Card JP (2004) Numerous GABAergic afferents to locus ceruleus in the pericerulear dendritic zone: Possible interneuronal pool. *J Neurosci* 24(9):2313–2321.
28. Zamalloa T, Bailey CP, Pineda J (2009) Glutamate-induced post-activation inhibition of locus coeruleus neurons is mediated by AMPA/kainate receptors and sodium-dependent potassium currents. *Br J Pharmacol* 156(4):649–661.
29. Ennis M, Aston-Jones G (1986) Evidence for self- and neighbor-mediated post-activation inhibition of locus coeruleus neurons. *Brain Res* 374(2):299–305.
30. Fegley DB, et al. (2008) Increased fear- and stress-related anxiety-like behavior in mice lacking tuberoinfundibular peptide of 39 residues. *Genes Brain Behav* 7(8):933–942.
31. Vong L, et al. (2011) Leptin action on GABAergic neurons prevents obesity and reduces inhibitory tone to POMC neurons. *Neuron* 71(1):142–154.
32. Madisen L, et al. (2010) A robust and high-throughput Cre reporting and characterization system for the whole mouse brain. *Nat Neurosci* 13(1):133–140.
33. Sousa VH, Miyoshi G, Hjerling-Leffler J, Karayannis T, Fishell G (2009) Characterization of Nkx6-2-derived neocortical interneuron lineages. *Cereb Cortex* 19(Suppl 1):i1–i10.
34. Kuo J, Usdin TB (2007) Development of a rat parathyroid hormone 2 receptor antagonist. *Peptides* 28(4):887–892.
35. Kutner RH, Zhang XY, Reiser J (2009) Production, concentration and titration of pseudotyped HIV-1-based lentiviral vectors. *Nat Protoc* 4(4):495–505.
36. Lois C, Hong EJ, Pease S, Brown EJ, Baltimore D (2002) Germline transmission and tissue-specific expression of transgenes delivered by lentiviral vectors. *Science* 295(5556):868–872.
37. Furukawa N, Saito M, Hakoshima T, Kohno K (2006) A diphtheria toxin receptor deficient in epidermal growth factor-like biological activity. *J Biochem* 140(6): 831–841.
38. Atasoy D, Aponte Y, Su HH, Sternson SM (2008) A FLEX switch targets Channelrhodopsin-2 to multiple cell types for imaging and long-range circuit mapping. *J Neurosci* 28(28):7025–7030.
39. Cecchini S, Virag T, Kotin RM (2011) Reproducible high yields of recombinant adeno-associated virus produced using invertebrate cells in 0.02- to 200-liter cultures. *Hum Gene Ther* 22(8):1021–1030.
40. Dixon WJ (1965) Up-and-down method for small samples. *J Am Stat Assoc* 60:967–978.
41. Chaplan SR, Bach FW, Pogrel JW, Chung JM, Yaksh TL (1994) Quantitative assessment of tactile allodynia in the rat paw. *J Neurosci Methods* 53(1):55–63.
42. Hylden JL, Wilcox GL (1980) Intrathecal morphine in mice: A new technique. *Eur J Pharmacol* 67(2-3):313–316.
43. Malmberg AB, Basbaum AI (1998) Partial sciatic nerve injury in the mouse as a model of neuropathic pain: Behavioral and neuroanatomical correlates. *Pain* 76(1-2): 215–222.
44. Dimitrov E, Usdin TB (2010) Tuberoinfundibular peptide of 39 residues modulates the mouse hypothalamic-pituitary-adrenal axis via paraventricular glutamatergic neurons. *J Comp Neurol* 518(21):4375–4394.